Operational Modal Analysis and Rational Finite-Element Model Selection for Ten High-Rise Buildings based on On-Site Ambient Vibration Measurements

Yun Zhou, Ph.D.[1]; Yi Zhou[2]; Weijian Yi, Ph.D.[3]; Taiping Chen[4]; Dexian Tan[5]; and Site Mi[6]

Abstract: The frequencies and mode shapes of high-rise buildings obtained from on-site ambient vibration testing and operational modal analysis (OMA) are very important for dynamic structural analysis and seismic design. This paper introduces a high-rise building ambient vibration test project in Laibin. Some results obtained from full-scale measurements of the dynamic behavior of 10 high-rise buildings are described. Different pre- and postprocessing techniques were used for ambient vibration signal analysis, from which the modal parameters were obtained using three OMA techniques. By rationally analyzing and modeling the stiffness of the infill walls, six finite element (FE) models were built in *PKPM* and *SAP2000* to estimate the analytical modal information. The influences of the infill wall mass and stiffness on the dynamic properties of a high-rise building are further discussed. According to the identified and calculated results, all three modes emerged in each modal dense region in the frequency domain of high-rise buildings. Finally, based on 25 proposed empirical equations, the fundamental periods of 10 buildings are calculated and summarized. **DOI: 10.1061/(ASCE)CF.1943-5509.0001019.**

Author keywords: High-rise building; Ambient vibration; Operational modal analysis; Infill wall stiffness; Fundamental period estimation.

Introduction

In recent decades, modern high-rise buildings have become more flexible and lightly damped because of the innovative structural forms and high-strength materials that are now used. Predicting the dynamic response of a building under ambient excitation (e.g., microtremors, wind, traffic) is increasingly important for both safety and serviceability design. However, ambient excitation cannot be directly measured; the structural responses are generally available for system identification via operational modal analysis (OMA). Thus, field measurements may provide a great opportunity for measuring the dynamic characteristics and responses of a high-rise building and comparing them with the design values (Xu et al. 2003). Field measurement results can also be used to improve model test techniques and to refine the numerical models used for structural analysis (Brownjohn and Pan 2008; Shi et al. 2012). Other potential applications include monitoring structural health, assessing seismic vulnerability, and evaluating comfort maintenance and structural vibration control (Satake et al. 2003).

Many full-scale on-site vibration tests have been conducted on high-rise buildings to record wind and structural response data (Kijewski-Correa et al. 2006), to study the influence of various modeling aspects on predicted dynamic properties and computer seismic response behavior (Maison and Neuss 1985), and to study the influence of wind on the performance of high-rise buildings (Li et al. 2006, 2011). Creating mathematical models of dynamic structural systems based on measured data also has significant potential for ambient vibration (Brownjohn 2003). The dynamic performance of a building can be estimated more accurately using finite-element (FE) models that are built based on measured data. Furthermore, comprehensive ambient vibration survey and FE model updating has provided a thoroughly validated analytical structural model (Brownjohn 2003). To identify the dynamic properties of a building, different output-only modal identification techniques, such as the random decrement technique (RDT), the Hilbert–Huang transform method (HHT), and stochastic subspace identification (SSI), can be applied to ambient and forced vibration measurements (Shi et al. 2012).

Correlation of dynamic characteristics from field measurements with FE analysis of tall buildings has rarely been carried out because of its complexity and the different sources of uncertainties. Infill walls are a typical type of nonstructural element in high-rise buildings that usually increase the stiffness of a building and are generally neglected in a priori FE models. Infill walls are considered only when their influence is suspected to be detrimental to overall structural response. However, in some cases these walls also introduce various undesirable effects on building performance. There are generally two modeling approaches for estimating local and global responses: micromodeling and macromodeling, respectively. The idea of macroelements was originally presented by Holmes (1961). Then, Saneinejad and Hobbs (1995) proposed an "equivalent strut model" for masonry frames with infill walls. Asteris et al. (2011) presented a review of the different macromodels used to analyze

[1]Associate Professor, College of Civil Engineering, Hunan Univ., Changsha 410082, Hunan, China; Hunan Provincial Key Lab on Damage Diagnosis for Engineering Structures, Hunan Univ., Changsha 410082, Hunan, China (corresponding author). E-mail: zhouyun05@gmail.com

[2]Postgraduate Student, Hunan Univ., Changsha 410082, China. E-mail: zhouyi1992@hnu.edu.cn

[3]Professor, Hunan Univ., Changsha 410082, China. E-mail: hunuyi2006@gmail.com

[4]Postgraduate Student, Hunan Univ., Changsha 410082, China. E-mail: 1587536480@qq.com

[5]Ph.D. Student, Hunan Univ., Changsha 410082, China. E-mail: springwind5206@sina.com

[6]Master, Hunan Univ., Changsha 410082, China. E-mail: 27809673@qq.com

Note. This manuscript was submitted on July 21, 2016; approved on November 29, 2016; published online on March 17, 2017. Discussion period open until August 17, 2017; separate discussions must be submitted for individual papers. This paper is part of the ***Journal of Performance of Constructed Facilities***, © ASCE, ISSN 0887-3828.

Table 1. Descriptions of the 10 Tested High-Rise Buildings

Number	Building name	Height (m)	Stories	Structural form	Temperature (°C)	10-min average wind speed (m/s)
1	Shui Hu Huang Men 1# (SH 1#)	116	39	Shear wall	16.2–17.9	0.8873
2	Shui Hu Huang Men 2# (SH 2#)	98	33	Shear wall	10.0–11.2	1.4723
3	Shui Yang Ren Jia 7# (SY 7#)	122	40	Shear wall	10.7–11.6	1.3229
4	Jin Sui Xiao Qu 1# (JS 1#)	99	34	Frame-shear wall	18.2–18.4	2.9373
5	Jin Sui Xiao Qu 3# (JS 3#)	116	41	Frame-shear wall	22.5–26.3	1.9880
6	Xiang Yun Yuan A# (XY A#)	75	24	Shear wall	12.0–12.8	2.8490
7	Xiang Yun Yuan B# (XY B#)	75	24	Shear wall	14.8–16.5	1.7169
8	Bei An Ya Ge 1# (BA 1#)	88	29	Shear wall	10.1–10.3	1.6856
9	Bei An Ya Ge 2# (BA 2#)	79	26	Shear wall	14.0–15.6	2.3767
0	Xiang Ge Li La 1# (XG 1#)	97	32	Frame-shear wall	11.7–13.5	0.6929

Note: Buildings 1–3, 4–5, 6–7 and 8–9 are, respectively, located in independent residential regions.

infilled frames. An alternative method for macromodeling is to model the infill panels using plane elements. Conversely, micromodeling simulates infill panels using detailed mesh to study the stress and strain distributions in a local region. Asteris et al. (2013) provided a thorough overview of the different micromodels proposed for analyzing infilled frames.

This paper introduces a full-scale high-rise building ambient vibration testing project in Laibin launched by Hunan University. Specifically, the following content is presented: (1) a detailed introduction to the project; (2) the performance of full-scale on-site ambient vibration testing and modal parameter identification of ten high-rise buildings using different OMA methods; (3) an investigation of rational modeling for infill panels and correlation of the building model characteristics with measurement results; (4) further discussion of the influences of infill wall mass and stiffness on the dynamic properties of a high-rise building based on the calibrated models; and (5) an evaluation and correlation of the measured fundamental periods of 10 buildings with those predicted using empirical equations.

Laibin High-Rise Building Test Project

Project Introduction

In 2013, a partnership between Structural Health Monitoring Research Team in Hunan University (www.hnutest.com) and the Laibin Housing and Urban-Rural Construction Committee was established to initiate a full-scale high-rise building ambient vibration test project in Laibin. This project allowed researchers to conduct a series of full-scale dynamic experiments and performance evaluations for high-rise buildings. A total of 10 high-rise buildings were carefully selected in five different residential regions. Detailed information on the tested buildings is given in Table 1; pictures and layout of the 10 high-rise buildings are shown in Fig. 1. All the tested buildings had been constructed within the previous three years and were designed according to the Chinese seismic design code provision GB 50011-2001 (Chinese Architectural and Building Press 2001). The tested buildings had no live loads of residents or furniture. The soil comprised slightly dense gravel and coarse or medium sand; therefore, most of the buildings used straight RC artificial excavating piles.

Experimental Setup (Laibin, Guangxi Autonomous Region, China)

An individual ambient vibration experiment was conducted on each tested building. Each building was equipped with a similar instrumentation layout that featured four US Wilcoxon 731A high-sensitivity accelerometers (adjustable sensitivity of 10, 100, or 1,000 V/g, frequency range of 0.05–450 Hz, and precision of 0.1 Hz) with a Wilcoxon Model P31 power supplier and four Chinese KD12000L accelerometers (sensitivity of 20 V/g, frequency range of 0.05–400 Hz, and precision of 0.1 Hz). These devices are capable of measuring acceleration at ultralow frequencies with high precision, making them well suited for measuring large-scale massive structures. The accelerometers were mounted in orthogonal pairs at three opposite corners along two sides of each building, with two accelerometers installed along the lateral direction and two installed along the orthogonal lateral direction. Four accelerometers were fixed and were located on the reference layer, and another four were installed on the moving layer. The reference layer was arranged at approximately the middle height of the building to conserve cable length, whereas the moving layer was set every three to five stories by moving the four accelerometers.

The typical instrumentation layout of Jin Sui Xiao Qu 3# is shown in Fig. 2. The sampling frequency for capturing ambient vibration signals was set to 204.8 Hz, and the signals in the time domain were recorded using an LMS Cadax 8-channel data acquisition (DAQ) system. The DAQ was programmed to continuously capture 15–20 min signals in the time domain to ensure that each independent test could be finished in one day. Because of budget limitations, wind speed was simply tested on the top of the building using a CIMAAR856 handheld anemometer and thermometer, which collected the 10-min average wind speed via measurements in the morning, at noon, and in the afternoon.

Signal Analysis and Processing

Data Quality Check and Processing Methods

After the ambient vibration signals were tested in the time domain, a data quality check was conducted to ensure reliable data for further analysis. The quality of the data was evaluated by visually inspecting the raw time-domain signals for each channel. A fast Fourier transformation (FFT) was also computed from the raw time-domain signal from each output channel during this step. The time- and frequency-domain signals for each channel were examined to identify any noisy or malfunctioning sensors. The spurious responses in the time history of each channel were removed to preserve the maximum number of acceptable responses.

OMA for ambient vibration signals includes frequency-domain, time-domain, and time- and frequency-domain approaches. In many previous applications, compared with analytical models, a number of missing modes or sporadic modes appeared or disappeared depending on the various pre- and postprocessing techniques used. The reasons for such modes and the reliability of intermittent modes are fundamental questions that continue to be challenges in

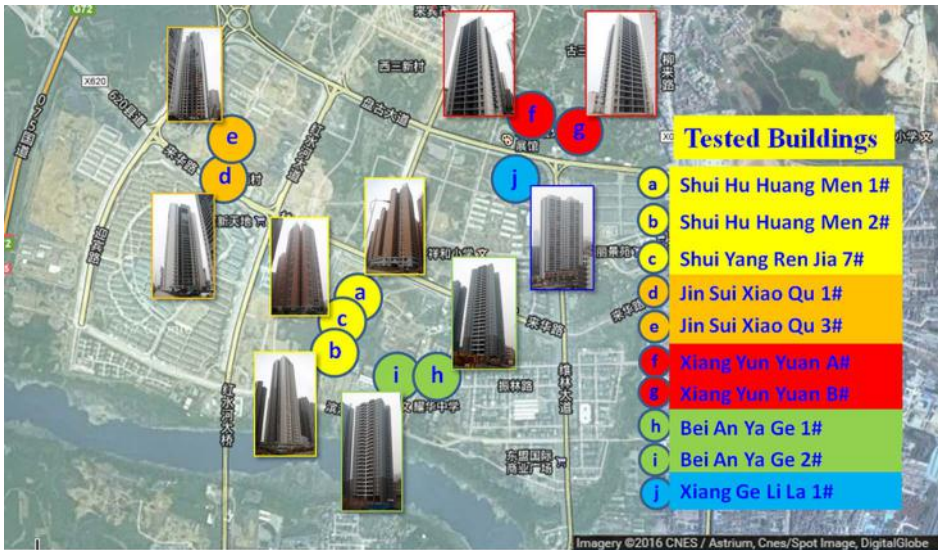

Fig. 1. Pictures and layout of the 10 tested buildings (images by Yun Zhou; Map Data: Google, Imagery ©2016 CNES/Astrium, CNES/Spot Image, DigitalGlobe): (a) SH 1#; (b) SH 2#; (c) SY 7#; (d) JS 1#; (e) JS 3#; (f) XY A#; (g) XY B#; (h) BA 1#; (i) BA 2#; (j) XG 1#

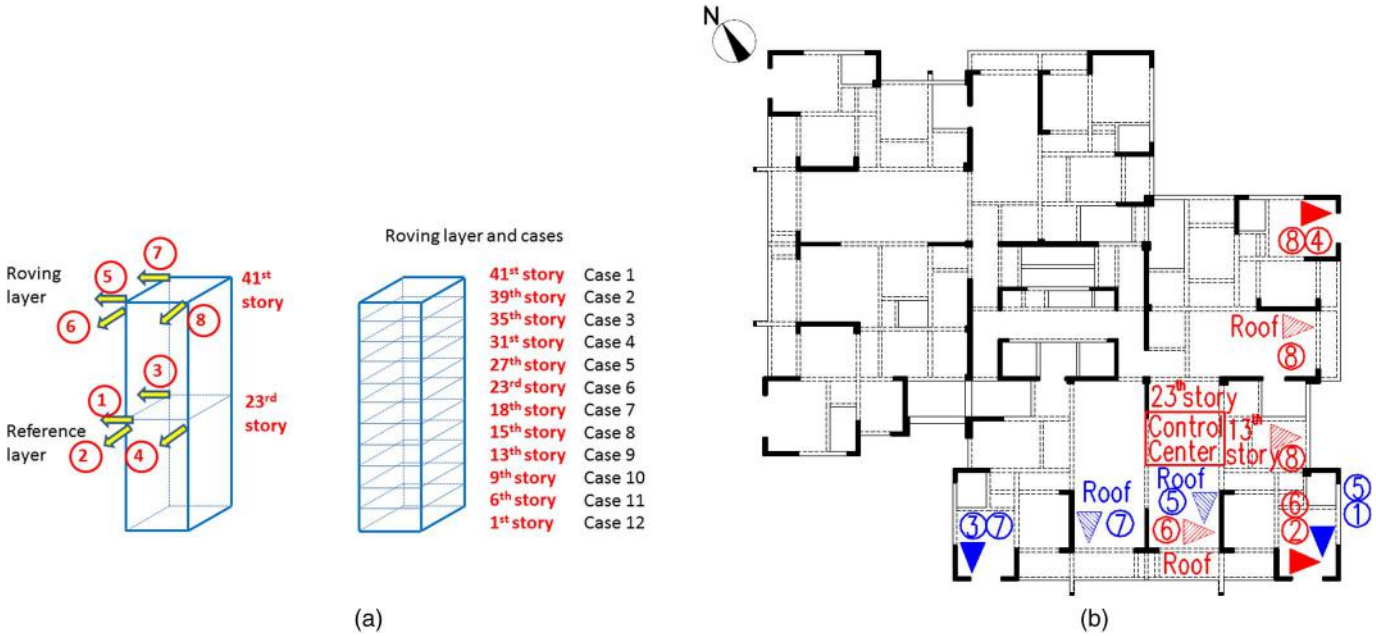

Fig. 2. Instrumentation layout for Jin Sui Xiao Qu 3#: (a) case definition in an elevation drawing; (b) instrumentation layout in plan

OMA (Ciloglu et al. 2012). To eliminate the influence of epistemic uncertainty, different pre- and postprocessing methods were used. Averaging time series data to generate pseudo-impulse response functions (p-IRFs) is a critical step in output-only modal analysis. To examine the influence of different averaging approaches, two different techniques were employed: random decrement (RD) functions and correlation functions. To prevent leakage, an exponential window was applied to the impulse response functions before postprocessing. Then the signals were transferred into the frequency domain using discrete Fourier transform (DFT).

To examine the influence of various modal parameter identification approaches, two approaches were included in the experimental program: the complex mode indicator function algorithm (CMIF) (Shih et al. 1989; Phillips et al. 1998) and SSI (Peeters 2000). The CMIF method operates in the spatial domain and involves the singular value decomposition (SVD) of a multiple-reference frequency response function matrix. The SSI method uses a state-space modeling approach and a two-stage process to extract modal parameters from time-domain data. In this research, the signals were pre- and postprocessed using three different paths, as shown in the flowchart in Fig. 3.

Cross-Correlation Technique

Cross-correlation functions describe the correlation between random variables at two different points in time. The auto- (R_{xx}) and cross- (R_{xy}) correlation functions used in this research are defined in Eqs. (1) and (2) (Allemang 1999; Ciloglu et al. 2012):

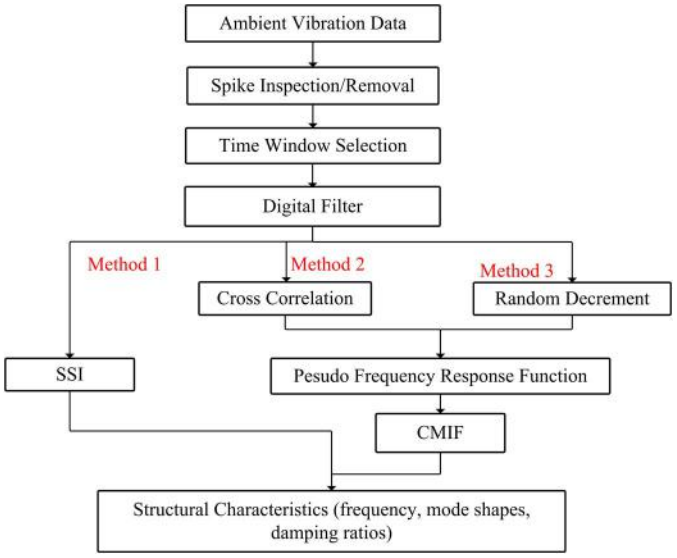

Fig. 3. Flowchart of signal processing

$$R_{XX}(\tau) = \frac{1}{N-\tau}\sum_{i=1}^{N-\tau} x(t_i)x(t_i+\tau) \tag{1}$$

$$R_{XY}(\tau) = \frac{1}{N-\tau}\sum_{i=1}^{N-\tau} x(t_i)y(t_i+\tau) \tag{2}$$

The length of a time block was considered to be 8,192 in the averaging process.

RD Method

The RD method, developed by Cole (1968), is a technique that transforms a random time series into a free decay of the measured structure. The basis of the technique is the selection of the trigger point. Asmussen (1997) proposed four triggering conditions: (1) level crossing; (2) local extremum; (3) positive point; and (4) zero crossing with positive slope triggering. In zero crossing triggering, the point at which the process crosses the zero line with a positive slope is the trigger point:

$$T_X^Z = \{X(t) = 0, \dot{X}(t_i) > 0\} \tag{3}$$

$$RD_{XX}(\tau) = \frac{1}{N}\sum_{i=1}^{N} x(t_i+\tau)|\{x(t_i) = 0, \dot{x}(t_i) > 0\} \tag{4}$$

$$RD_{YX}(\tau) = \frac{1}{N}\sum_{i=1}^{N} y(t_i+\tau)|\{x(t_i) = 0, \dot{x}(t_i) > 0\} \tag{5}$$

where $x(t)$ and $y(t)$ = realizations of $X(t)$ and $Y(t)$, respectively.

CMIF Method

The CMIF method is a zero-order spatial domain algorithm. Additional details of this method and the necessary equations were described by Shih et al. (1989) and Phillips et al. (1998). The basis of the CMIF method is the SVD of a traditional multiple-reference function (FRF) matrix. In this method, the SVD of the FRF matrix is performed at every spectral line, and the following matrix equation is obtained:

$$[H(j\omega)] = [U(j\omega)][\sum(j\omega)][V(j\omega)]^H \tag{6}$$

where $[H(j\omega)]$ = FRF matrix; $[U(j\omega)]$ = left singular matrix; $[\sum(j\omega)]$ = diagonal singular value matrix; and $[V(j\omega)]$ = right singular matrix. The CMIF method is an enhanced basic peak-picking procedure, and the frequency resolution affects the accuracy of the identified frequency.

SSI Method

A time-domain identification method, SSI identifies the modal properties of a system from only the output (ambient vibration). Additional details of this method were given by Peeters (2000). The basic premise is that the physical model used to describe the continuous dynamic behavior of a system can be expressed as an equivalent discrete-time stochastic state-space model given by

$$x_{k+1} = Ax_k + w_k \tag{7}$$

$$y_k = Cx_k + v_k \tag{8}$$

where x_k = discrete state vector; w_k = process noise (the disturbances and the unknown excitation); A = state transition matrix, which completely characterizes the dynamics of the system by its eigenvalues; y_k = sampled output vector; v_k = measurement noise (due to the sensors and the unknown excitation); C = output matrix, which determines how the internal states are transferred to the external world; and k = time instant.

Signal Processing Results

As mentioned previously, the signals were pre- and postprocessed using three different methods, as shown in the flowchart in Fig. 3. The operational mode shapes were extracted from the combination of the ambient vibration signals of the moving layer and the reference layer; then the different cases were integrated via sensors on the reference layer. The stabilization figure produced by Method 1 is shown in Fig. 4(a). The SVD figures obtained by Method 2 and Method 3 are presented in Figs. 4(b and c), respectively. The 12 modal periods and damping ratios identified by Method 1 are presented in Table 2, and the modal periods identified by Method 2 and Method 3 are listed in Table 3. These tables show that although some modes were missing when Method 1 was used, the other two methods were able to identify relatively complete modal information as a supplement. For Jin Sui Xiao Qu 3#, the first 12 mode shapes identified by Method 1 are shown in Fig. 5. In each building, all three modes emerged in each modal dense region, and each region generally included two orthotropic lateral swaying modes and one torsional mode. Because of the inconsistencies in the mass center and the stiffness center in most of the high-rise buildings, the two orthotropic lateral swaying modes always included a torsional mode component to a certain extent.

FE Modeling

A range of representative three-dimensional (3D) FE models of the buildings were constructed to estimate structural modes. Shear walls can be modeled using various types of FE model, such as the warping single-column model, the plane stress model, or shell element model (Smith and Coull 1991). The beams and columns used frame elements, and the floors were constructed using a shell element.

In this research, two different types of software were used to construct the FE models for eigenvalue analysis. First, the *SATWE*

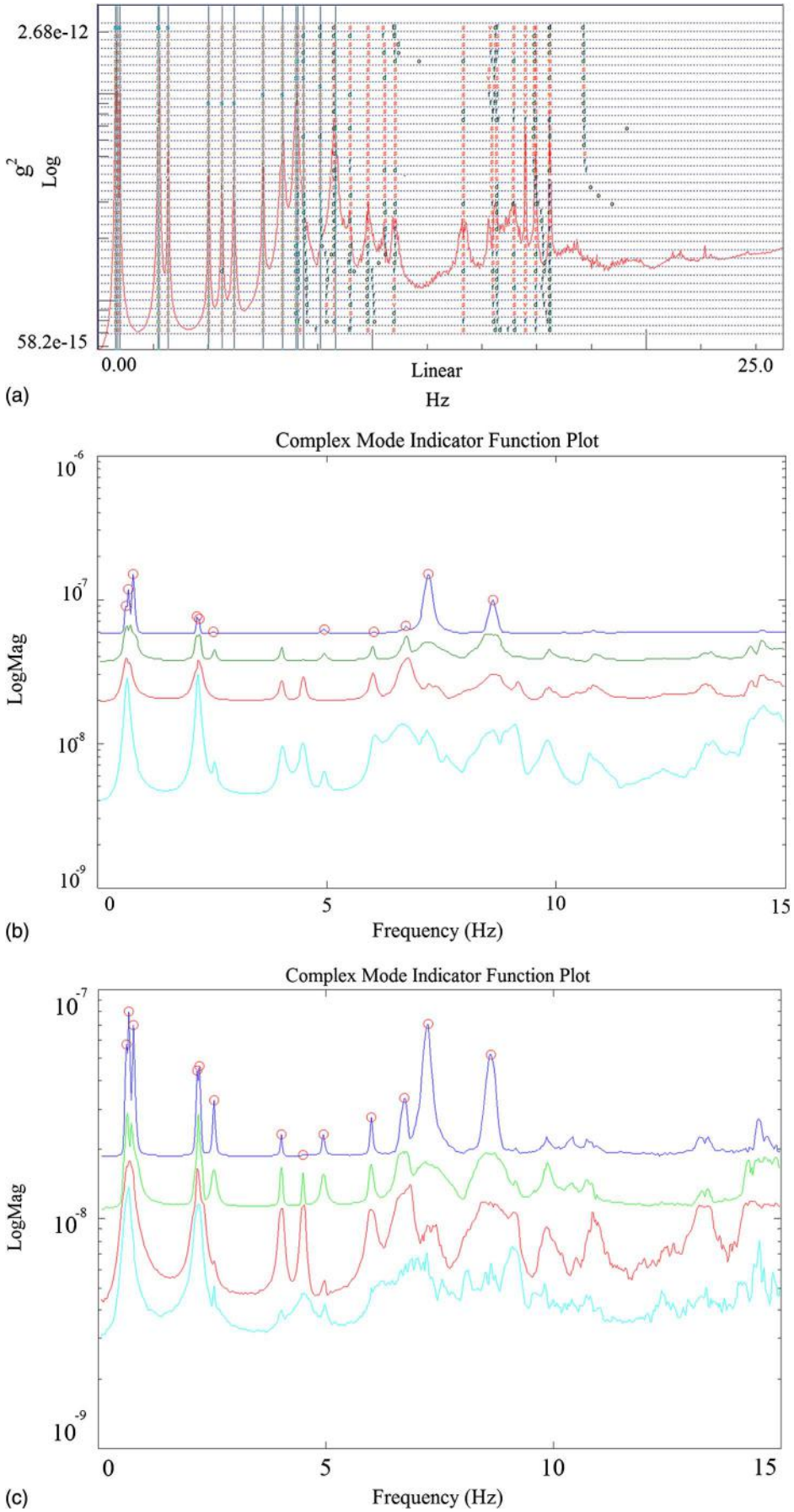

Fig. 4. Signal processing results for Jin Sui Xiao Qu 3#: (a) stabilization figure using Method 1; (b) SVD figure using Method 2; (c) SVD figure using Method 3

Table 2. 12 Identified Modal Periods and Damping Ratios for the 10 Buildings Using Method 1

		1	2	3	4	5	6	7	8	9	10
Mode	Dynamic property	SH#	SH2#	SY7#	JS1#	JS3#	XYA#	XYB#	BA1#	BA2#	XG1#
1st	Period	1.786	1.433	1.626	—	1.621	0.917	0.918	1.412	1.245	1.724
	Damp.	0.36%	1.28%	2.29%	—	0.37%	0.46%	0.32%	0.65%	0.41%	5.17%
2nd	Period	1.560	1.294	1.443	1.183	1.479	0.865	0.865	1.195	1.122	1.414
	Damp.	0.99%	3.38%	10.55%	0.27%	0.47%	0.36%	0.35%	0.39%	0.35%	3.75%
3rd	Period	0.529	1.214	1.266	—	1.287	0.800	0.788	1.040	0.958	0.979
	Damp.	0.85%	2.14%	0.03%	—	0.33%	0.43%	0.96%	0.33%	0.39%	0.69%
4th	Period	—	0.392	—	—	0.459	0.259	0.261	0.362	0.328	0.392
	Damp.	—	0.59%	—	—	0.41%	0.48%	0.47%	0.47%	0.36%	0.48%
5th	Period	0.487	0.360	0.415	0.406	0.450	0.255	0.258	0.345	0.319	0.367
	Damp.	0.42%	0.94%	0.42%	0.20%	0.43%	0.65%	0.37%	0.39%	0.44%	0.40%
6th	Period	0.443	0.354	0.367	0.384	0.393	0.240	0.243	0.314	0.280	0.334
	Damp.	0.44%	0.68%	0.34%	0.87%	0.41%	1.22%	0.88%	0.32%	0.33%	0.95%
7th	Period	0.246	0.203	0.202	0.193	0.248	0.139	—	—	0.170	0.202
	Damp.	1.25%	0.82%	0.70%	0.78%	0.41%	0.68%	—	—	0.49%	0.87%
8th	Period	0.187	0.185	0.193	0.180	0.222	—	—	0.182	0.157	—
	Damp.	0.71%	0.92%	0.73%	0.50%	0.60%	—	—	1.58%	1.99%	—
9th	Period	—	0.173	0.183	—	0.202	0.132	0.136	0.164	0.142	0.181
	Damp.	—	1.57%	0.35%	—	0.55%	0.18%	2.18%	1.02%	0.69%	1.60%
10th	Period	0.168	0.139	—	0.144	0.167	0.128	0.099	—	0.113	0.126
	Damp.	0.46%	0.89%	—	0.89%	0.43%	0.53%	0.72%	—	1.11%	3.17%
11th	Period	0.157	0.124	0.132	—	0.149	0.098	0.091	0.122	0.103	0.118
	Damp.	0.38%	1.24%	1.35%	—	0.94%	0.80%	0.87%	1.43%	0.50%	1.71%
12th	Period	—	0.112	0.123	0.128	0.138	0.091	0.087	0.107	0.100	0.106
	Damp.	—	1.05%	0.26%	0.80%	0.85%	1.94%	0.86%	1.31%	0.81%	0.86%

Table 3. 12 Identified Modal Periods for the 10 Buildings Using Method 2 and Method 3

		1	2	3	4	5	6	7	8	9	10
Mode	Method	SH1#	SH2#	SY7#	JS1#	JS3#	XYA#	XYB#	BA1#	BA2#	XG1#
1st	Method 2	1.812	1.572	1.597	1.312	1.486	0.873	0.917	—	1.245	1.592
	Method 3	1.761	1.600	1.534	1.312	1.618	0.843	0.919	1.397	1.227	1.590
2nd	Method 2	1.718	—	—	1.307	1.468	0.870	0.903	1.193	1.125	1.517
	Method 3	1.639	—	1.362	1.307	1.484	0.810	0.917	1.104	1.122	1.546
3rd	Method 2	—	—	1.332	—	1.290	0.855	0.827	1.038	1.005	1.272
	Method 3	—	—	1.287	—	1.479	0.804	0.787	1.038	0.983	1.536
4th	Method 2	—	0.393	0.424	0.408	0.458	0.258	0.261	0.361	0.319	0.384
	Method 3	—	0.381	—	0.407	0.459	0.258	0.276	0.362	0.328	0.398
5th	Method 2	0.487	—	0.422	0.402	0.454	—	0.260	0.346	0.319	0.379
	Method 3	0.488	0.359	0.415	0.403	0.451	—	0.254	0.362	0.320	0.386
6th	Method 2	—	0.355	0.369	0.370	0.393	0.247	—	0.314	0.279	0.371
	Method 3	0.447	—	0.367	0.353	0.425	0.243	0.245	0.313	0.280	0.380
7th	Method 2	0.237	—	0.200	0.202	—	—	0.170	—	0.171	—
	Method 3	0.247	0.239	0.207	0.203	0.252	0.136	0.151	—	0.171	0.222
8th	Method 2	—	—	0.191	0.191	—	0.132	0.151	—	0.139	—
	Method 3	0.245	0.181	0.186	0.182	—	0.133	0.138	—	0.153	—
9th	Method 2	—	—	0.188	0.183	0.204	0.129	0.136	—	—	—
	Method 3	0.203	—	0.180	0.182	0.211	0.132	0.137	0.165	0.139	0.174
10th	Method 2	0.168	—	0.132	0.145	0.139	—	0.100	0.126	0.113	—
	Method 3	0.168	—	0.131	0.146	0.168	0.131	0.098	0.127	0.113	0.139
11th	Method 2	0.163	—	0.131	—	0.138	—	0.093	—	0.100	0.119
	Method 3	0.155	—	0.130	0.131	0.138	0.099	0.091	0.107	0.103	0.119
12th	Method 2	0.136	—	0.123	0.128	0.138	0.090	0.088	—	0.099	—
	Method 3	0.137	—	0.121	0.128	0.138	0.091	0.088	0.102	0.102	0.115

module in *PKPM* was used. Widely employed for building design in China, PKPM is based on the Chinese building design code. In this software, when a high-rise building is modeled, the mass of the infill walls is considered to load the corresponding beam without influencing the stiffness of the structure. Because the stiffness of infill walls is neglected in the model, a 0.7–1.0 fundamental period reduction factor was considered in this research for calculating seismic response behavior. Because *PKPM* is limited to Chinese building design, *SAP2000* was used for the modeling process; *SAP2000* is used for engineering research worldwide. This software is a fully integrated program that allows quick modeling, convenient modification, and powerful analysis functions for 3D structures, such as elastic static analysis and time-history analysis. It includes the national design codes for most countries, including China.

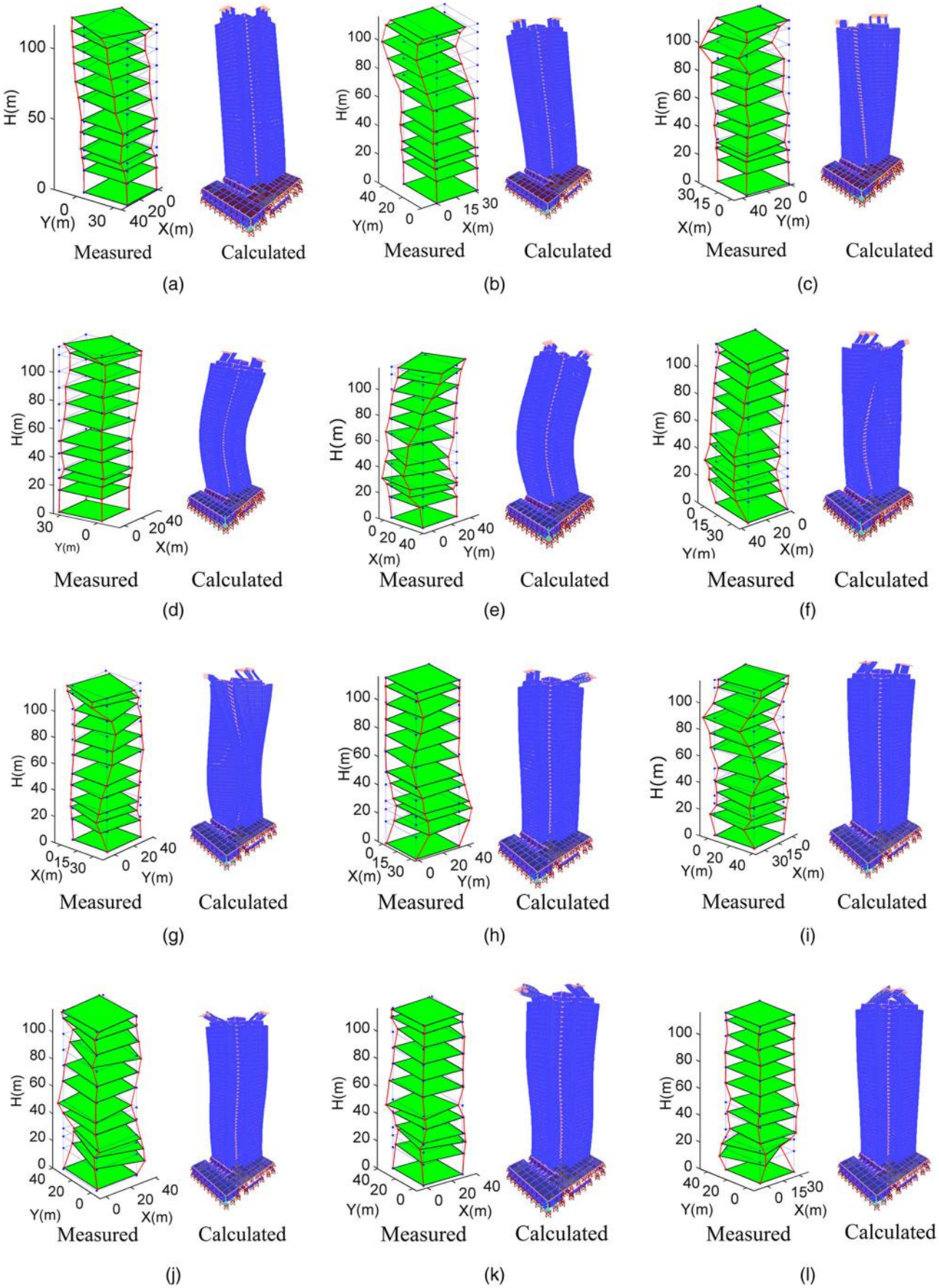

Fig. 5. Comparison of the first 12 measured and calculated modes for the Jin Sui Xiao Qu 3# building (using Method 1 and Model 3): (a) Mode 1 (Y); (b) Mode 2 (X); (c) Mode 3 (T); (d) Mode 4 (Y); (e) Mode 5 (X); (f) Mode 6 (T); (g) Mode 7 (Y); (h) Mode 8 (X); (i) Mode 9 (T); (j) Mode 10 (Y); (k) Mode 11 (X); (l) Mode 12 (T); $X/Y = X/Y$ direction lateral swaying modes, respectively; T = torsional mode)

Table 4. Six Different FE Modeling Methods

Model	Stiffness	Mass	Software
Model 1	No	Yes	*SATWE* in *PKPM*
Model 2	No	Yes	*SAP2000*
Model 3	Yes (shell element)	Yes	*SAP2000*
Model 4	Yes (diagonal strut)	Yes	*SAP2000*
Model 5	Yes (shell element)	No	*SAP2000*
Model 6	No	No	*SAP2000*

In general, infill walls are considered only in the gravity direction as an additional dead load. However, infill walls affect the rigidity of the structure and also increase the total mass of the structure, consequently increasing the inertial forces on the structure in an earthquake. Infill walls may cause adverse effects on the frame elements by creating short columns, torsion, or stiffness irregularities (Kose and Karslioglu 2009). The shell element is generally used to model the infill walls as long as its physical parameters are rational. Another typical infill wall model is simulated as diagonal struts connected to four diagonal corners, where each strut is activated only under a compressive force. Determining the effective width w of the equivalent diagonal struts is essential for this approach. Various methods have been developed to evaluate the effective width of a diagonal strut for infilled frames without openings by Mainstone (1971), Paulay and Priestly (1992), and Fardis (2009). The Mainstone model (1971) was adopted to simulate infill walls with openings. Thus, the effective width of the equivalent diagonal struts is given by Eq. (9):

$$w_w = \frac{0.175 L_w}{\cos\theta (\lambda H_c)^{0.4}} \tag{9}$$

$$\text{where } \lambda = \sqrt[4]{\frac{E_w I_w \sin(2\theta)}{4 E_c I_c H_w}} \tag{10}$$

in which t_w = infill panel thickness; H_c = column height; L_w and H_w = clear horizontal and vertical dimensions of the masonry wall, respectively; θ = inclination angle of the diagonal element to the horizontal; l_c = second moment of inertia of the column (in the normal direction to the infill wall); and E_c and E_w = moduli of elasticity of the concrete column and the infill wall, respectively.

In this research, the compressive strength of the infill walls, which comprise MU10 brick (with a compressive strength of 10 MPa) and M5 mortar (with a compressive strength of 5 MPa), was 2.4 MPa. To evaluate the influence of different modeling approaches for the infill walls on the dynamic properties of the high-rise buildings, six different FE models were built for comparison, as shown in Table 4. Model 1 was built in *PKPM* and is a typical design model used in China. The uniformly distributed load produced by the infill walls was assumed to be added onto the corresponding beam, whereas the stiffness of the infill walls was taken into account by a 0.7–1.0 fundamental period reduction factor in seismic analysis according to GB 50011-2001 (China Architectural and Building Press 2001). Model 2 was designed as the baseline reference model in *SAP2000*, which is convenient for comparison of different modeling approaches.

Models 1 and 2 are designed to compare modeling errors via different FE model software programs. For Model 3 and Model 4, the stiffness influence of the infill walls was modeled using a shell element and diagonal struts, respectively. In the FE analysis, the elastic modulus of the parameter was used to simulate the infill wall. Because the measured modes differed from the calculated modes, the modal information measured by ambient vibration was used to calibrate the FE model. A trial-and-error calculation process was performed to generate the optimized elastic modulus of the infill wall and the width of the diagonal strut to match the measured modes.

The first 12 modes that were measured and calculated for the 10 high-rise buildings are shown in Fig. 6. After calibration, the modal parameters calculated using Models 3 and 4 were quite close to the measured modes, which demonstrated that both infill wall–modeling strategies can be used for high-rise building modeling. As an example, the 12 modes calculated using the calibrated Model 3 for Jin Sui Xiao Qu 3# are shown in Fig. 5 and compared with the measured modes using Method 1.

Based on the previous discussions, the influences of the infill wall mass and stiffness on the dynamic properties of a high-rise building are further discussed through two additional models: Model 5, which considered only the influence of stiffness, and Model 6, which neglected the influences of both mass and stiffness. The comparison of the 12 modes for the 10 buildings is shown in Fig. 7. Both Model 1 (considering only mass) and Model 6 (considering neither mass nor stiffness) overestimated the measured natural period and were approximately two to three times greater than the measured value. The value calculated by Model 5 (considering only stiffness) was slightly smaller than the measured value. Therefore, it can be concluded that infill wall mass has a greater effect on the dynamic properties of a high-rise building than infill wall stiffness.

Fundamental Period Analysis

The fundamental period, which is strongly related to distributions of mass and stiffness, is a basic dynamic property of a high-rise building and the most important parameter related to seismic design. Per Chinese code, the mode-superposition response spectrum method was used for seismic evaluation of the 10 buildings tested in Laibin. In the analysis, the seismic influence coefficient is strongly related to the fundamental period, which is related to a few influence factors, such as the configuration of the planar structure, the distributions of mass and stiffness, and the material properties and distribution of the nonstructure. The empirical equations for calculating the dynamic properties of buildings have been provided by many institutes and universities and are related to a few basic pieces of information and characteristics, including building height, number of stories, building plan dimensions, structural type, and foundation type. In this research, 25 empirical equations were retrieved from the literature and are included in Table 5.

Based on the proposed empirical equations, the fundamental periods of the 10 buildings were calculated (Fig. 8). In the figure, a histogram represents the distribution of the fundamental period calculated by the proposed empirical equations. The lateral axis denotes fundamental period, and the vertical axis denotes frequency; the height of each rectangle represents the frequency of the corresponding period range. The mean value of the proposed empirical equations is compared with the measured value. The measured fundamental period of each building lies in the general range of the values estimated by different empirical equations; finally, the measured values are shown to be smaller than the average value of the 25 equations. One reason for this difference could be that the measured fundamental period was obtained under ambient excitation—that is, the measured period of the structure under wind, traffic, and microtremor influence. In addition, some relevant factors, such as nonstructural components and soil-structure interaction, that affect the calculation period are neglected in the

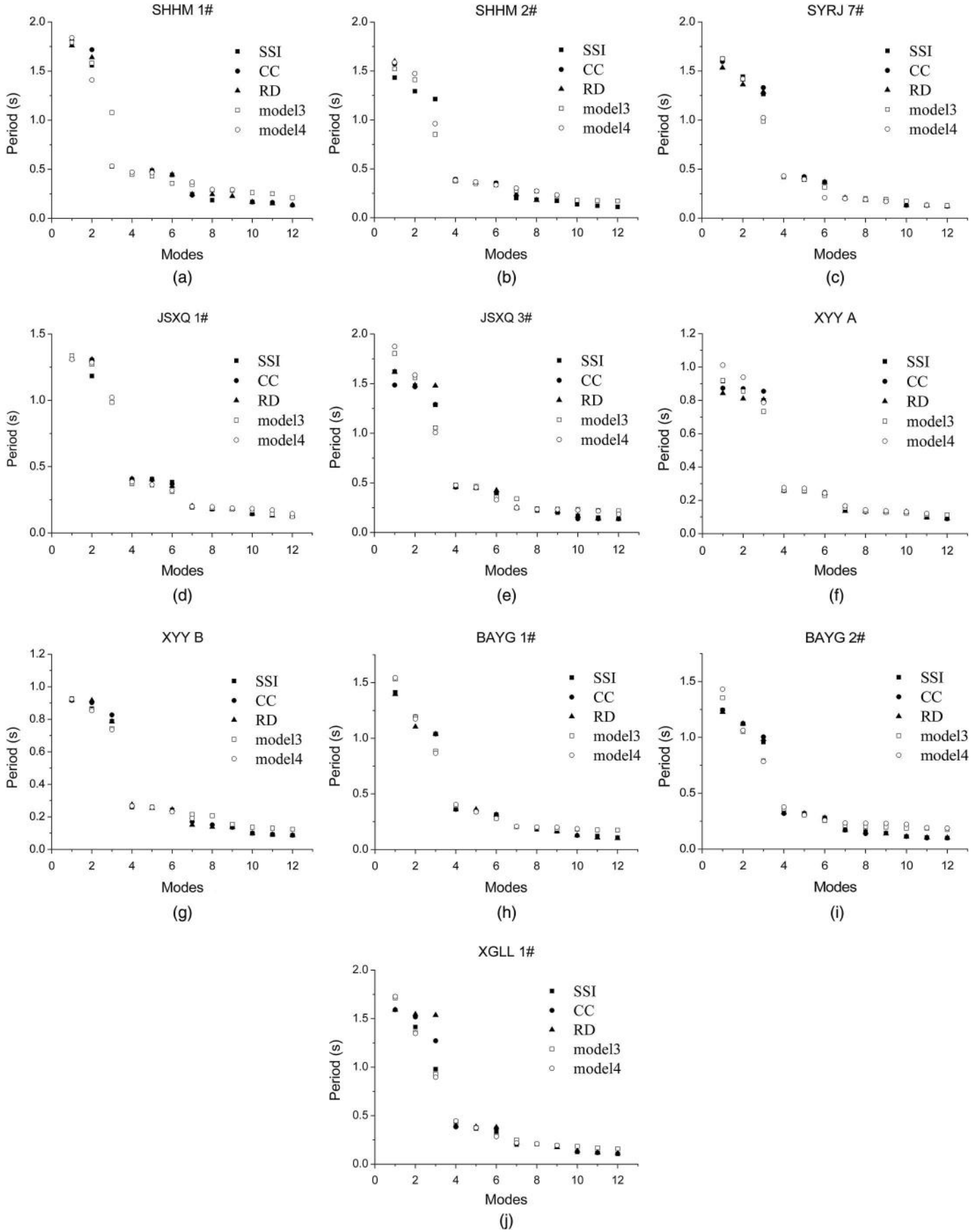

Fig. 6. Comparison of the measured and calibrated models for the 10 buildings: (a) SH 1#; (b) SH 2#; (c) SY 7#; (d) JS 1#; (e) JS 3#; (f) XY A#; (g) XY B#; (h) BA 1#; (i) BA 2#; (j) XG 1#

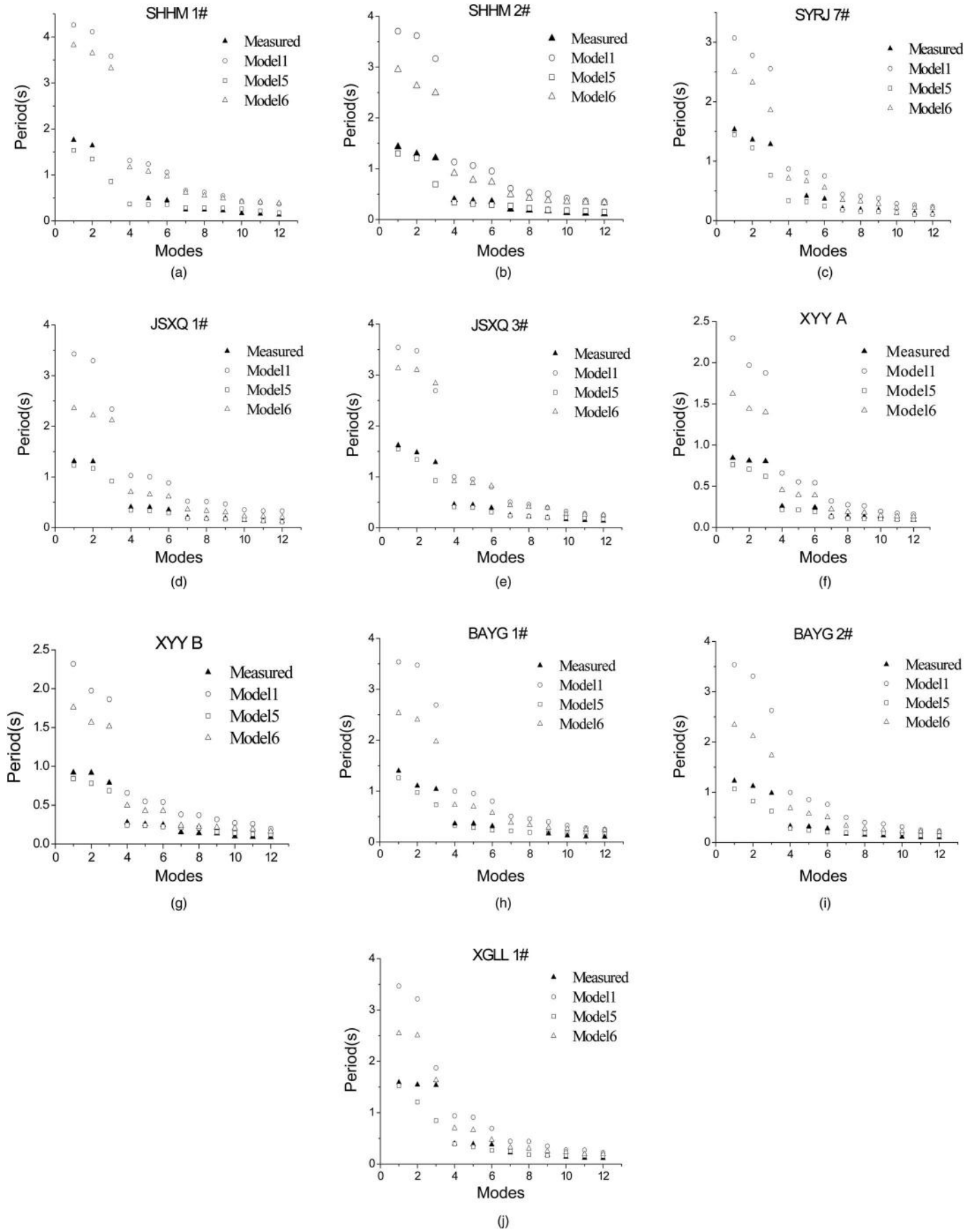

Fig. 7. Comparison of the measured values and calculated values of Models 1, 5, and 6: (a) SH 1#; (b) SH 2#; (c) SY 7#; (d) JS 1#; (e) JS 3#; (f) XY A#; (g) XY B#; (h) BA 1#; (i) BA 2#; (j) XG 1#

Table 5. Empirical Equations Used to Estimate the Fundamental Periods of High-Rise Buildings

Number	Equation	Range of application
1 (NRCC 2005)	$T = 0.05h^{0.75}$	Based on measured periods of buildings
2 (Gilles 2011)	$T = 0.019h$	Regression analysis to test goodness of fit of different equations of the mean-value curve
3 (Chopra and Goel 2000)	$T = 0.015h$	Calculates design base shear and predicts concrete shear wall buildings; building height <270 m
4 (Chopra and Goel 2000)	$T = 0.025h$	Calculates seismic displacements; building height <270 m
5 (Hong and Hwang 2000)	$T = 0.0294h_n^{0.804}$	Predicts median fundamental vibration period of RC moment resisting frame (MRF) building with given height
6 (UBC 1997)	$T = 0.0731h_n^{0.75}$	Evaluates fundamental vibration period of RC MRF building
7 (Goel and Chopra 1997)	$T = 0.0507h_n^{0.92}$	Obtains measured periods of RC MRF buildings in California using unconstrained regression analysis
8 (CEN 2004)	$T_{EC8} = 0.075H^{0.75}$	According to the European seismic design regulations; only for RC structures
9 (Goel and Chopra 1997)	$T_{G-C} = 0.053H^{0.9}$	For RC structures
10 (Hatzigeorgiou and Kanapitsas 2013)	$T = 0.073H^{0.745}$	Considers influence of infill and concrete shear walls, soil flexibility, and building height
11 (UBC 1970)	$T = 0.05h_n/D^{0.5}$	According to 1970 edition of Uniform Building Code
12 (ASCE 2006)	$T = 0.0724H^{0.8}$	General buildings
13 (Baeza 1963)	$T = 0.035n$	Typical Chilean building code; developed from study of 42 structures with 4–17 stories
14 (Midorikawa 1990)	$T = 0.049n$	Based on study of 117 structures with 3–30 stories
15 (Goel and Chopra 1997)	$T = 0.0466H^{0.9}$	Based on lower bound of data; proposed for RC frames
16 (Crowley and Pinho 2010)	$T = 0.09H/D^{0.5}$	Vibration of RC moment resisting frames with rigid infills
17 (BIS 1984)	$T = 0.1n$	Earthquake-resistant design of structures
18 (NRC 1995)	$T = 0.1N$	Based on National Building Code of Canada
19 (Crowley and Pinho 2006)	$T = 0.38H$	Equations for calculating period of uncracked infilled buildings using weighted mean period of vibration for each frame
20 (Navarro et al. 2007)	$T = (0.049 \pm 0.01)N$	Microtremor measurements at top of 39 RC buildings with 2–9 stories using three-component seismometer
21 (Guler et al. 2008)	$T = 0.026H^{0.9}$	Relationship between height and fundamental period of vibration of Turkish RC moment resisting frames with 4–12 stories from ambient vibrations
22 (Gallipoli et al. 2010)	$T = 0.016H$	Best statistical result; building height 1–20 stories
23 (Michel et al. 2010)	$T = 0.013H = 0.039N$	RC and masonry buildings
24 (Pan et al. 2014)	$T = 0.0927N^{0.8183}$	RC and masonry buildings
25 (Panzera et al. 2013)	$T_{(S)} = 0.018H^{0.928}$	Mainly masonry buildings

Note: D = building dimension; h, h_n, H = total building height above ground; n, N = number of stories.

calculation because of simplifications of the mathematical model. Another reason could be that the most unfavorable load used in the calculation is usually larger than the actual building weight, making the measured fundamental period smaller than the calculated period.

Conclusions

A full-scale ambient vibration test project was discussed in this paper. Full-scale ambient vibration tests were conducted on 10 buildings in downtown Laibin; three different OMA methods were then successfully implemented to generate modal frequencies and mode shapes. For comparison with the measured modal results, six *PKPM* and *SAP2000* FE models were created for the high-rise buildings to investigate the proper modeling method, especially for infill walls. To demonstrate the rationality of the measured results, the measured fundamental periods were compared with the empirical estimation results. The following main conclusions can be drawn.

First, few results have been reported for detailed ambient vibration tests conducted on a number of high-rise buildings in a city. In this project, at least two similar buildings in each residential district were chosen as the test objects, and the results can be used to compare the dynamic characteristics in a local region.

Second, because of the epistemic uncertainty that exists in the signal processing procedure, the SSI method was also used for OMA, and the cross-correlation and RD methods, followed by the CMIF method, were then used for further comparison. The advantage of using different methods is the ability to identify missing modes that result from using any single method. According to the results, modal dense region was found in the frequency domain of the high-rise buildings. In one modal dense region, two lateral swaying modes and one torsional mode were observed. Because of inconsistencies in the mass and stiffness centers, the lateral swaying modes were always combined with torsional modes.

Third, six different FE models were built in *PKPM* and *SAP2000*, and after calibration the shell element model and diagonal strut model were shown to rationally simulate the infill walls. The modes estimated by *PKPM* (the typical design model used in China) underestimated the measured modes, which were also reliable because they fell within the range of the periods estimated from 25 empirical equations. Based on the calibrated models, the influences of infill wall mass and stiffness on the dynamic properties of a high-rise building were further investigated. It was found that infill wall mass affects the dynamic properties of a high-rise building more than infill wallsstiffness.

Finally, based on the 25 proposed empirical equations, the fundamental periods of 10 buildings were calculated and summarized here. The mean value of the proposed empirical equations was compared with the measured value. The measured fundamental period of each building fell in the range of values estimated by different empirical equations, whereas the measured values were less than the average value of the 25 equations. One reason for this could be that the measured fundamental period of buildings is obtained under ambient excitation, meaning that under conditions of wind, traffic, and microtremors. In addition, some other relevant factors, such as nonstructural components and soil-structure

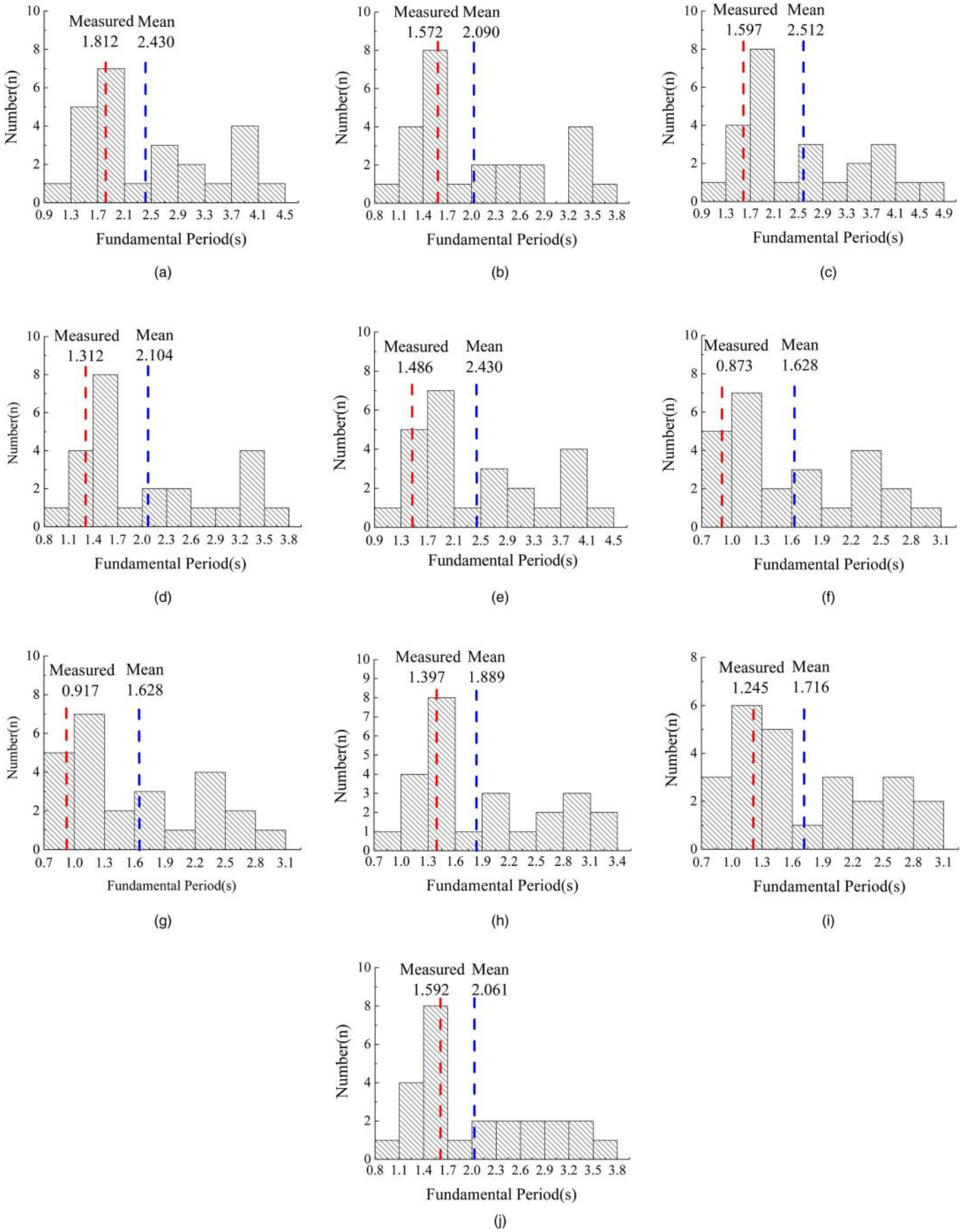

Fig. 8. Comparison of the measured fundamental periods with the calculated values: (a) SH 1#; (b) SH 2#; (c) SY 7#; (d) JS 1#; (e) JS 3#; (f) XY A#; (g) XY B# (h) BA 1#; (i) BA 2#; (j) XG 1#

interaction, that affect the calculation period were neglected in the calculation to simplify the mathematical model. Another reason could be that the most unfavorable load used in the calculation is usually larger than the actual building weight so that the measured fundamental period is smaller than the calculated period.

Acknowledgments

The authors are grateful for the support provided for this research by the National Key Research and Development Program of China (No. 2016YFC0701400), the NSFC (No. 51208190), the Hunan Provincial Natural Science Foundation of China (No. 12JJ4053), and the Research Fund for Chinese Doctoral Program of Higher Education (No. 20120161120028).

References

Allemang, R. J. (1999). "Vibrations: Analytical and experimental modal analysis." Structural Dynamics Research Laboratory, Univ. of Cincinnati, Cincinnati.

ASCE. (2006). "Minimum design loads for buildings and other structures." *ASCE/SEI 7-05-2006*, Reston, VA.

Asmussen, J. C. (1997). "Modal analysis based on the random decrement technique—Application to civil engineering structures." Ph.D. thesis, Univ. of Aalborg, Aalborg, Denmark.

Asteris, P. G., Antoniou, S. T., Sophianopoulos, D. S., and Chrysostomou, C. Z. (2011). "Mathematical macromodeling of infilled frames: State of the art." *J. Struct. Eng.*, 10.1061/(ASCE)ST.1943-541X.0000384, 1508–1517.

Asteris, P. G., Cotsovos, D. M., Chrysostomou, C. Z., Mohebkhah, A., and Al-Chaar, G. K. (2013). "Mathematical micromodeling of infilled frames: State of the art." *Eng. Struct.*, 56, 1905–1921.

Baeza, M. (1963). "Natural periods of reinforced concrete buildings." Engineering thesis, Dept. of Civil Engineering, Univ. of Chile, Santiago, Chile.

BIS (Bureau of Indian Standards). (1984). "Criteria for earthquake resistant design of structures." New Delhi, India.

Brownjohn, J. M. (2003). "Ambient vibration studies for system identification of tall buildings." *Earthquake Eng. Struct. Dyn.*, 32(1), 71–95.

Brownjohn, J. M., and Pan, T. C. (2008). "Identifying loading and response mechanisms from ten years of performance monitoring of a tall building." *J. Perform. Constr. Facil.*, 10.1061/(ASCE)0887-3828(2008)22:1(24), 24–34.

CEN (European Committee for Standardization). (2004). "Design of structures for earthquake resistance—Part 1." *Eurocode 8*, Brussels.

China Architectural and Building Press. (2001). "Code for seismic design of buildings." *GB 50011-2001*, Beijing.

Chopra, A. K., and Goel, R. K. (2000). "Building period formulas for estimating seismic displacements." *Earthquake Spectra*, 16(2), 533–536.

Ciloglu, K., Zhou, Y., Moon, F., and Aktan, A. (2012). "Impacts of epistemic uncertainty in operational modal analysis." *J. Eng. Mech.*, 10.1061/(ASCE)EM.1943-7889.0000413, 1059–1070.

Cole, H. A. (1968). "On-the-line analysis of random vibrations." *Paper No. 68-288*, American Institute of Aeronautics and Astronautics, Reston, VA.

Crowley, H., and Pinho, R. (2006). "Simplified equations for estimating the period of vibration of existing buildings." *Proc., 1st European Conf. on Earthquake Engineering and Seismology*, European Association for Earthquake Engineering (EAEE), Geneva.

Crowley, H., and Pinho, R. (2010). "Revisiting Eurocode 8 formulae for periods of vibration and their employment in linear seismic analysis." *Earthquake Eng. Struct. Dyn.*, 39(2), 223–235.

Fardis, M. N. (2009). *Seismic design, assessment and retrofitting of concrete buildings: Based on EN-Eurocode 8*, Springer, Dordrecht, Netherlands.

Gallipoli, M. R., et al. (2010). "Empirical estimates of dynamic parameters on a large set of European buildings." *Bull. Earthquake Eng.*, 8(3), 593–607.

Gilles, D. (2011). "In situ dynamic characteristics of reinforced concrete shear wall buildings." Ph.D. thesis, Dept. of Civil Engineering and Applied Mechanics, McGill Univ., Montréal.

Goel, R. K., and Chopra, A. K. (1997). "Period formulas for moment-resisting frame buildings." *J. Struct. Eng.*, 10.1061/(ASCE)0733-9445(1997)123:11(1454), 1454–1461.

Guler, K., Yuksel, E., and Kocak, A. (2008). "Estimation of the fundamental vibration period of existing RC buildings in Turkey utilizing ambient vibration records." *J. Earthquake Eng.*, 12(S2), 140–150.

Hatzigeorgiou, G. D., and Kanapitsas, G. (2013). "Evaluation of fundamental period of low-rise and mid-rise reinforced concrete buildings." *Earthquake Eng. Struct. Dyn.*, 42(11), 1599–1616.

Holmes, M. (1961). "Steel frames with brickwork and concrete infilling." *Proc. Inst. Civ. Eng.*, 19(4), 473–478.

Hong, L. L., and Hwang, W. (2000). "Empirical formula for fundamental vibration periods of reinforced concrete buildings in Taiwan." *Earthquake Eng. Struct. Dyn.*, 29(3), 327–337.

Kijewski-Correa, T., et al. (2006). "Validating wind-induced response of tall buildings: Synopsis of the Chicago full-scale monitoring program." *J. Struct. Eng.*, 10.1061/(ASCE)0733-9445(2006)132:10(1509), 1509–1523.

Kose, M. M., and Karslioglu, O. (2009). "Effects of infills on high-rise buildings: A case study." *Struct. Des. Tall Spec. Build.*, 18(8), 907–920.

Li, Q. S., et al. (2006). "Wind tunnel and full-scale study of wind effects on China's tallest building." *Eng. Struct.*, 28(12), 1745–1758.

Li, Q. S., Zhi, L., Tuan, A. Y., Kao, C., Su, S., and Wu, C. (2011). "Dynamic behavior of Taipei 101 tower: Field measurement and numerical analysis." *J. Struct. Eng.*, 10.1061/(ASCE)ST.1943-541X.0000264, 143–155.

Mainstone, R. J. (1971). "On the stiffness and strength of infilled frames." *Proc. Inst. Civ. Eng.*, 49(2), 57–90.

Maison, B. F., and Neuss, C. F. (1985). "Dynamic analysis of a forty-four story building." *J. Struct. Eng.*, 10.1061/(ASCE)0733-9445(1985)111:7(1559), 1559–1572.

Michel, C., Guéguen, P., Lestuzzi, P., and Bard, P. (2010). "Comparison between seismic vulnerability models and experimental dynamic properties of existing buildings in France." *Bull. Earthquake Eng.*, 8(6), 1295–1307.

Midorikawa, S. (1990). "Ambient vibration tests of buildings in Santiago and Viña del Mar." *Rep. No. 90-1*, Pontificia Universidad Catolica de Chile, Escula de Ingenieria, Departamento de Ingenieria Estructural, Santiago, Chile.

Navarro, M., et al. (2007). "Analysis of the weightiness of site effects on reinforced concrete (RC) building seismic behaviour: The Adra town example (SE Spain)." *Earthquake Eng. Struct. Dyn.*, 36(10), 1363–1383.

NRCC (National Research Council of Canada). (1995). "The National Building Code." Ottawa.

NRCC (National Research Council of Canada). (2005). "National Building Code of Canada." Ottawa.

Pan, T. C., Goh, K. S., and Megawati, K. (2014). "Empirical relationships between natural vibration period and height of buildings in Singapore." *Earthquake Eng. Struct. Dyn.*, 43(3), 449–465.

Panzera, F., Lombardo, G., and Muzzetta, I. (2013). "Evaluation of building dynamic properties through in situ experimental techniques and 1D modeling: The example of Catania, Italy." *Phys. Chem. Earth Parts A/B/C*, 63, 136–146.

Paulay, T., and Priestly, M. N. (1992). *Seismic design of reinforced concrete and masonry buildings*, Wiley, New York.

Peeters, B. (2000). "System identification and damage detection in civil engineering." Ph.D. dissertation, Katholieke Univ., Leuven, Belgium.

Phillips, A. W., Allemang, R. J., and Fladung, W. A. (1998). "The complex mode indicator function (CMIF) as a parameter estimation method." *Proc., 16th Int. Modal Analysis Conf.*, Society for Experimental Mechanics, Bethel, CT, 705–710.

PKPM. [Computer software]. Weifang City, China, Geil Weifang Steel Works, Ltd.

Saneinejad, A., and Hobbs, B. (1995). "Inelastic design of infilled frames." *J. Struct. Eng.*, 10.1061/(ASCE)0733-9445(1995)121:4(634), 634–650.

SAP2000. [Computer software]. CSI, Walnut Creek, CA.

Satake, N., Suda, K., Arakawa, T., Sasaki, A., and Tamura, Y. (2003). "Damping evaluation using full-scale data of buildings in Japan." *J. Struct. Eng.*, 10.1061/(ASCE)0733-9445(2003)129:4(470), 470–477.

Shi, W., Shan, J., and Lu, X. (2012). "Modal identification of Shanghai World Financial Center both from free and ambient vibration response." *Eng. Struct.*, 36, 14–26.

Shih, C. Y., Tsuei, Y. G., Allemang, R. J., and Brown, D. L. (1989). "Complex mode indication function and its applications to spatial domain parameter estimation." *Proc., 7th Int. Modal Analysis Conf.*, Society for Experimental Mechanics, Bethel, CT, 533–540.

Smith, B. S., and Coull, A. (1991). *Tall building structures: Analysis and design*, Wiley, New York.

UBC (Uniform Building Code). (1970). "International Conf. of building officials." Whittier, CA.

UBC (Uniform Building Code). (1997). "International Conf. of Building Officials." Whittier, CA.

Xu, Y. L., Chen, S. W., and Zhang, R. C. (2003). "Modal identification of Di Wang building under Typhoon York using the Hilbert-Huang transform method." *Struct. Des. Tall Spec. Build.*, 12(1), 21–47.